energies

MDPI

Article

The Nonuniform Distribution of Stylolite in Bioclastic Limestones and Its Influence on Reservoir Petro-Physical Properties—A Case Study of the Mishrif Formation from the Ah Oilfield

Jiacheng Xu [1], Ya Deng [1,*], Meiyan Fu [2], Rui Guo [1], Pei Chen [2], Guanghui Duan [2] and Ruicheng Ma [1]

[1] Research Institute of Petroleum Exploration & Development, PetroChina, Beijing 100083, China; xujiacheng@petrochina.com.cn (J.X.); grgr@petrochina.com.cn (R.G.); ruichengma@petrochina.com.cn (R.M.)
[2] Energy College, Chengdu University of Technology, Chengdu 610059, China; fumeiyan08@cdut.cn (M.F.); jackychen@stu.cdut.edu.cn (P.C.); 2021020202@stu.cdut.edu.cn (G.D.)
* Correspondence: dengya@petrochina.com.cn

Abstract: The effect of stylolite caused by the pressure dissolution process on the reservoir petro-physical properties is still controversial. This study aims to reveal the effect of stylolite on the porosity and permeability of packstone and wackestone in the Mishrif Formation from the Ah oilfield in the Middle East. Based on the observation of thin sections and cores, X-ray diffraction analysis and porosity and permeability measurement, the lithofacies, diagenesis and patterns of stylolites have been investigated. There are six lithofacies in the Mi4 member, including bivalve green algae packstone, green algae packstone, pelletoid green algae packstone, echinoderm packstone, rudist packstone, planktonic foraminifera wackestone and bioclastic wackestone. The mechanical compaction and pressure dissolution could be observed in these lithofacies, with the development of dissolution seams and stylolites. The density of stylolite has a relationship with the lithofacies and early cementation. The boundary between the echinoderm packstone and the green algae packstone mostly developed as stylolites. There are four types of stylolite on the cores. Type A is the wave-like stylolite developed at the boundary between the echinoderm packstones and green algae packstones. Type B is the zigzag stylolite with high amplitude in the green algae packstones. Type C is the stylolites with low amplitude in the bioclastic wackestones. Type D is the high-angle stylolite, which is oblique to the bedding plane. The permeability of reservoir rocks could be improved by dissolution along the type B stylolite, while the type A and type C stylolite have little effect on permeability. The permeability of green algae packstone and echinoderm packstone will decrease with the development of stylolites. The porosity and permeability of bivalve green algae packstone will decrease after stylolitization, resulting from the relatively high density of stylolite. The physical properties of bioclastic wackestone could be improved by the bioturbation and formation of stylolite. According to the analysis of production performance in the same lithofacies, the occurrence of stylolites could result in the development of oil baffles. This study could be extended to evaluate the effect of stylolite in carbonate reservoir rocks.

Keywords: stylolite; pressure dissolution; anticline; permeability; Mishrif Formation

Citation: Xu, J.; Deng, Y.; Fu, M.; Guo, R.; Chen, P.; Duan, G.; Ma, R. The Nonuniform Distribution of Stylolite in Bioclastic Limestones and Its Influence on Reservoir Petro-Physical Properties—A Case Study of the Mishrif Formation from the Ah Oilfield. *Energies* **2022**, *15*, 3032. https://doi.org/10.3390/en15093032

Academic Editor: Mofazzal Hossain

Received: 13 February 2022
Accepted: 6 April 2022
Published: 21 April 2022

1. Introduction

Stylolites are widely found in carbonate rocks and siliciclastic rocks. In 1751, Mylius compared the stylolites with silicified wood and named them "schwielen" for the first time [1]. Stylolites are mainly composed of host rock, a stylolite surface and a stylolite membrane. In general, stylolites could be baffles for fluid flow due to the existence of insoluble residues, without pore space and permeability [2–6]. A mathematical kinetic model has been established. It predicts that stylolite can form at roughly constant spacings,

and the bedding planes between beds with different texture are the focus of porosity instability, which can lead to the formation of a stylolite [7].

The influence of stylolite on the fluid flow capacity and reservoir petro-physical properties is ambiguous. In the process of burial diagenesis, a large number of dissolutions will form along the stylolites [8,9]. The column of stylolite could be a channel for fluid flow. However, most of the void spaces were filled by calcites or dolomites adjacent to the stylolites. As the product of pressure dissolution, the calcite or dolomite precipitated somewhere, postdating the calcium and magnesium ions, which were released into pore waters in the deep buried environment [10,11]. In particular, euhedral dolomite crystals are usually found along the stylolites [10]. It is suggested that the role of stylolite in the carbonate reservoir is positive, and the development of stylolite can improve the permeability [12]. As an important structural plane, stylolites constitute effective oil and gas migration channels, together with the fractures [13]. Stylolites are finer than fractures, with a higher degree of networking and three-dimensional connectivity than that of fractures [14]. In some cases, crude oil or asphalt could be found in the fractures and stylolites in the limestones [10,15,16]. Different types of stylolites could be identified on cores, as a response to pressure dissolution.

There are a large number of stylolites developed in the oil-bearing limestones from the Jurassic and Cretaceous in the Middle East, with equivocal effects on the permeability [8,13,17]. The effect of stylolites on the petro-physical properties of the reservoir is significant for oil exploitation. The lithofacies, paragenesis and the distribution of stylolites were studied in the Mishrif Formation, Ah Oilfield, in Central Iraq, using observations of thin sections, measurement of the permeability and porosity and XRD detection. Based on the research of the distribution and pattern of stylolites, the permeability on cores with different lithofacies near stylolites was analyzed. As a result, the impacts of stylolites on the petro-physical properties were discussed.

2. Geological Setting

Iraq is located on the unstable continental shelf in the north of the Persian Gulf Basin, on the northern margin of the ancient Gondwana continent [18]. The tectonic evolution of the Persian Gulf Basin was mainly affected by the Alpine tectonic movement. There are two large structural areas from west to east in Iraq, i.e., the stable shelf area in the west and the unstable shelf area in the east. The latter is mainly characterized by thick sedimentary rocks. The tectonic framework of the basement in Iraq is controlled by a series of NW-SE or NE-SW trending faults [18]. According to the degree of structural deformation, the unstable shelf area is further divided into various main zones and sub-zones. There are three main structural zones in the eastern unstable shelf area, i.e., the Mesopotamia zone, piedmont zone and fold deformation zone. The Mesopotamian belt can be subdivided into the Zubair sub-belt, Euphrates sub-belt and Tigris sub-belt [19].

Ah Oilfield is located in the middle of the Euphrates sub-belt of the Mesopotamian basin. The sediments in the Euphrates sub-belt are the thickest and most deeply buried, with a relatively stable structure in the Mesopotamia basin. Ah Oilfield is a huge, broad, long-axis anticline with three structural highs. The obduction of the Neo-Tethys Ocean in the Late Cretaceous might have resulted in the formation of an initial anticline. As a response to the Zagros Orogeny in the late Miocene and Pliocene, the anticline was compressed by the NW-SE tectonic stress [20]. The timing for the oil charging in the study area was the Late Cretaceous [20]. In the study, the southeastern structural high of the long-axis anticline is the research target. The stratigraphic column of the Cretaceous in the study area is shown in Figure 1A. The Cenomanian Mishrif Formation is overlaid by the Turonian Khasib Formation and is underlaid by the Rumaila Formation (Figure 1A). The Mishrif Formation in the oilfield is composed of limestones bearing various skeletal grains, with thickness of more than 100 m. The Mishrif Formation could be divided into five members, i.e., Mi1, Mi2, Mi3, Mi4 and Mi5. There are no drilling cores collected from the Mi1, Mi2, Mi3 members. The Mi5 member is composed of packstone with intensive cementation. The Mi4 member is an important oil-bearing zone in the oilfield, with relatively strong

heterogeneity vertically (Figure 1B). Furthermore, the Mi4 member could be divided into Mi4-1, Mi4-2, Mi4-3, Mi4-4 and Mi4-5 lithozones. Among the five zones, the Mi4-2 and Mi4-3 lithozones represent high-quality reservoirs. Based on the core description, the stylolites are pervasive in the Mi4 member (Figure 1B).

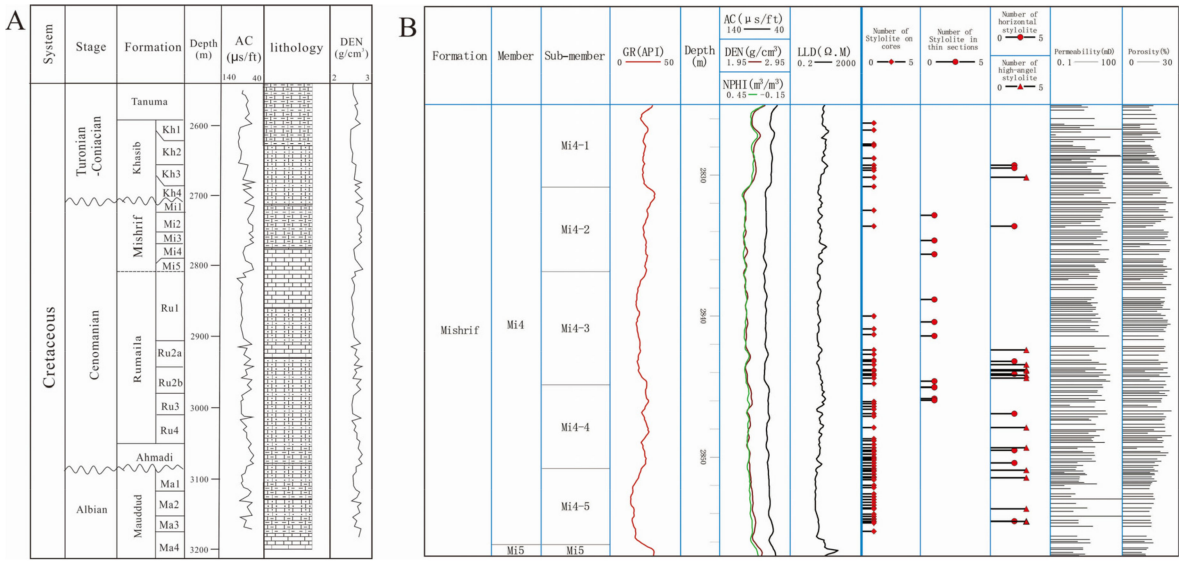

Figure 1. The stratigraphic column in the Ah Oilfield. (**A**) The stratigraphic column of Cretaceous; (**B**) The stratigraphic column of the Mi4 member of the Mishrif Formation.

3. Methods

There are three cored wells for the Mi4 member in the eastern high of Ah oilfield. Three core samples per meter of the Mi4 member have been collected. In total, 310 core samples and thin sections from the Mishrif Formation in Ah Oilfield have been described and identified. The sedimentary structure (including soft sediment deformation), lithological texture, color and oil-bearing property were analyzed based on the core description. Based on the casting thin section observation, the lithofacies and the pore types have been identified. Thin sections were examined for mineralogy using Alizarin Red staining. The composition of minerals was determined by using a Rigaku DMAX-3C X-ray diffractometer (Rigaku Corporation, Tokyo, Japan) equipped with Cu Kα radiation (40 kV, 20 mA). The porosity and permeability of the rock with stylolite have been tested on the cores, using the saturated alcohol and gas method [21].

4. Results

4.1. Lithofacies

The lithology of the Mi4 member is skeletal-rich packstone or wackestone. The skeletal grain and bioclast in these limestones include foraminifera, green algae, bivalve, echinoderm, rudist, oyster, etc. The non-skeletal grains include pelletoid, intraclast and a small amount of gravel-sized intraclast. The mineral composition of the Mi4 member was detected by XRD. Calcite is the most common in the composition of minerals, with minor dolomite (Table 1). There are very small amounts of terrigenous quartz in the limestones, with less than 1%. The lithofacies could be divided into bivalve green algae packstone, green algae packstone, pelletoid green algae packstone, echinoderm packstone, rudist packstone, planktonic foraminifera wackestone and bioclastic wackestone (Figure 2), etc. There are some cements in the internal cavities of the bioclast in the packstone or wackestone, including sparry calcite and autogenetic dolomite. There are many white patches observed on cores (Figure 3), which are packstones with very low porosity and permeability caused by intensive cementation. Bioturbation could be observed on the cores (Figure 3), which is characterized by the burrow filled by the echinoderm packstone. It

is reported that the bioturbation in the Cretaceous Khasib Formation in the study area is related to the activity of Callianassidae [22].

Table 1. The mineral composition of limestone from the Mi4 member.

Lithology	Depth (m)	Weight Percentage × 10^{-2}				
		Clay	Gypsum	Quartz	Calcite	Dolomite
Limestone	2797.84–2797.87	0	0	0.33	99.67	0
Limestone	2804.16–2804.19	0	0	0.28	99.16	0.56
Limestone	2812.08–2812.11	0	0	0.34	99.66	0
Limestone	2817.96–2817.99	0	0	0.35	95.17	4.48
Limestone	2835.30–2835.33	0	0	0.27	95.29	4.45
Limestone	2846.86–2846.89	0	0	0.48	98.46	1.07
Limestone	2849.53–2849.56	0	0	0	100	0
Limestone	2856.84–2856.87	0	0	0	93.45	6.55

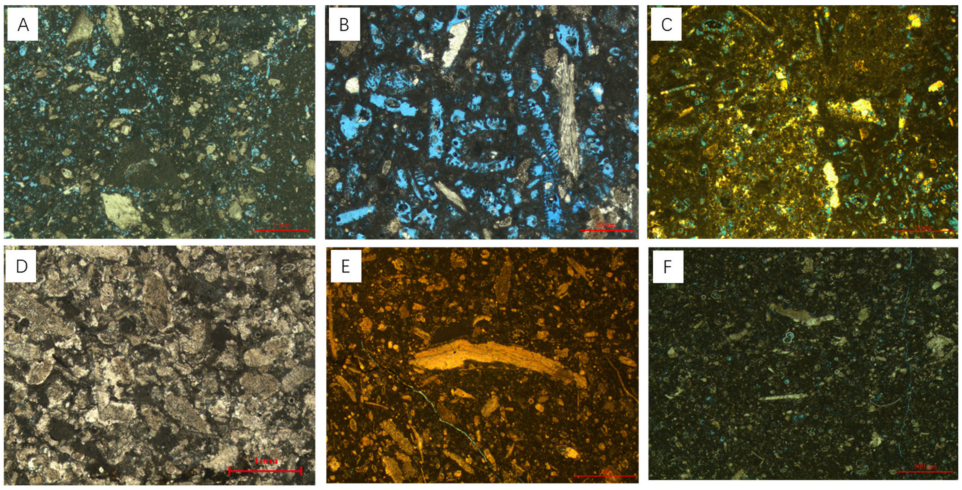

Figure 2. The lithofacies in the Mi4 member of the Mishrif Formation in Ah Oilfield. (**A**) Bivalve green algae packstone; (**B**) green algae packstone; (**C**). pelletoid green algae packstone; (**D**) echinoderm packstone; (**E**) bioclastic wackestone; (**F**) planktonic foraminifera wackestone.

Based on the observation of casting thin sections, the main void spaces of the limestones from the Mi4 member are pores, and a few unfilled fractures. The types of pores are mainly moldic pores (accounting for 11.31% in whole rock), non-fabric selective dissolved pores (accounting for 6.3% in whole rock), intragranular pores (accounting for 4.81% in whole rock), intrafossil pores (accounting for 3.29% in whole rock) and intercrystalline dissolved pores among the crystals of calcite in the matrix (accounting for 2% in whole rock). The distribution of pore types in the study area is related to lithofacies. A large number of intragranular pores, moldic pores and intrafossil pores are developed in the bivalve green algae packstone, green algae packstone and pelletoid green algae packstone. The intrafossil pores and intercrystalline dissolved pores among the crystals of calcite in the matrix are mainly developed in the bioclastic wackestone and planktonic foraminifera wackestone.

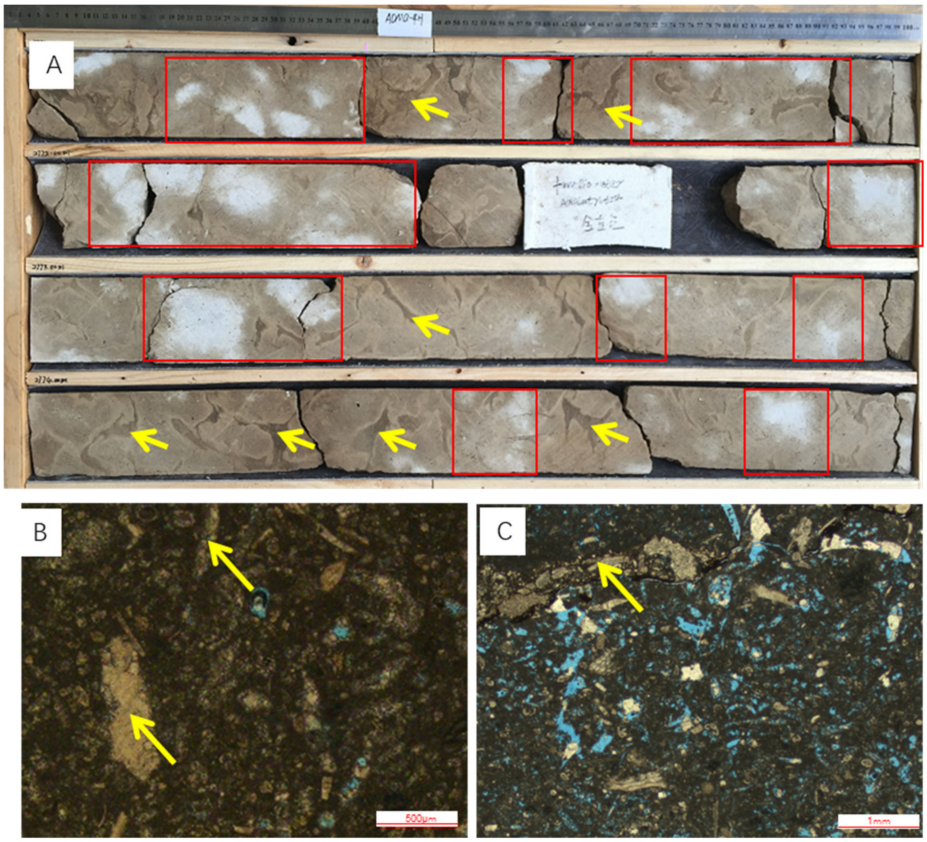

Figure 3. The white patches and burrows on cores and thin sections from the Mi4 member. (**A**) The white patches and burrows on cores; the white patches are shown in the red box and the burrows are shown by the yellow arrow; (**B**) image of a thin section from the white patch; there is intensive cementation by calcite; (**C**) image of a thin section from the boundary between a burrow and host rock; the burrow is filled by echinoderm packstone, marked by a yellow arrow.

4.2. Diagenesis Related to the Pressure Dissolution

The mechanical compaction and pressure dissolution in the limestones from the Mi4 member could be observed under thin sections. Machel (2004) and Railsback (1993) have reported that the pressure dissolution occurred at a burial depth beyond 1 km [23,24]. During the diagenesis, the pressure dissolution was correlated with the fracturing, dolomitization and dissolution. The paragenesis of diagenetic minerals is shown in Figure 4. In the early diagenesis, the dolomitization occurred in the wackestones with the reflux of medium-salinity brine in the inner ramp. With the sea level fall, the exposure of the sediments on shoals induced the micritization, fabric dissolution, neomorphism, authigenic dolomites precipitation, calcite cementation and overgrowth cementation of echinoderm in the mixed seawater–freshwater phreatic zone and later freshwater phreatic zone. At the lowest sea level, there was some weathering crack development and non-fabric dissolution at the freshwater vadose zone. Then, the weakly consolidated sediments were buried to experience mechanical compaction. After a depth of more than 1 km, intergranular pressure dissolution occurred, resulting in dissolution seams in the wackestones and fitted fabric in the packstones. Stylolite started to form when the rocks could no longer accommodate the increasing burial load [25]. Dolomitization could occur in the process of stylolite. Meanwhile, there was slight non-fabric dissolution and meso-coarse crystalline calcite cementation in the late diagenesis. As a response to the compressional stress caused by the late tectonic movement, some tectonic fractures formed in the limestones from the Mi4 member.

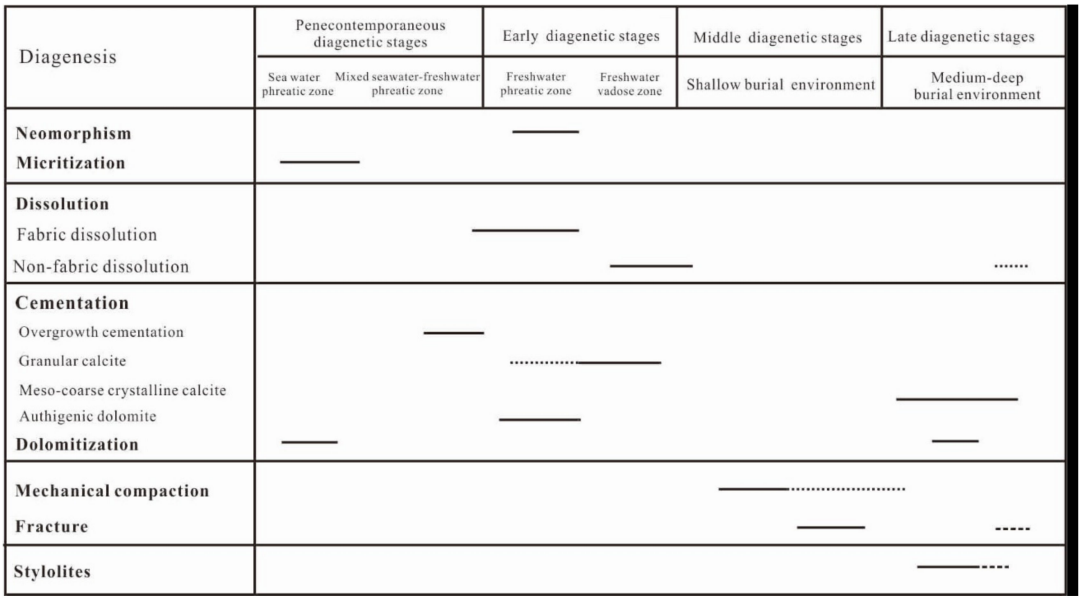

Figure 4. The paragenesis of the limestones from the Mi4 member in the Ah Oilfield.

Most fracturing occurred before pressure dissolution, with evidence from petrography. As shown in Figure 5A, the weathering cracks with irregular shape were cut by a stylolite, predating the pressure dissolution. The dolomites occurred within the insoluble residue of a dissolution seam (Figure 5D), resulting from the Mg^{2+} from the clay minerals with pressure dissolution. The dissolution could be seen at the column of the stylolite, which is shown in Figure 5E. The diagenetic fluid flowed along the column of the stylolite, leading to the formation of void spaces, which occurred in the late diagenesis.

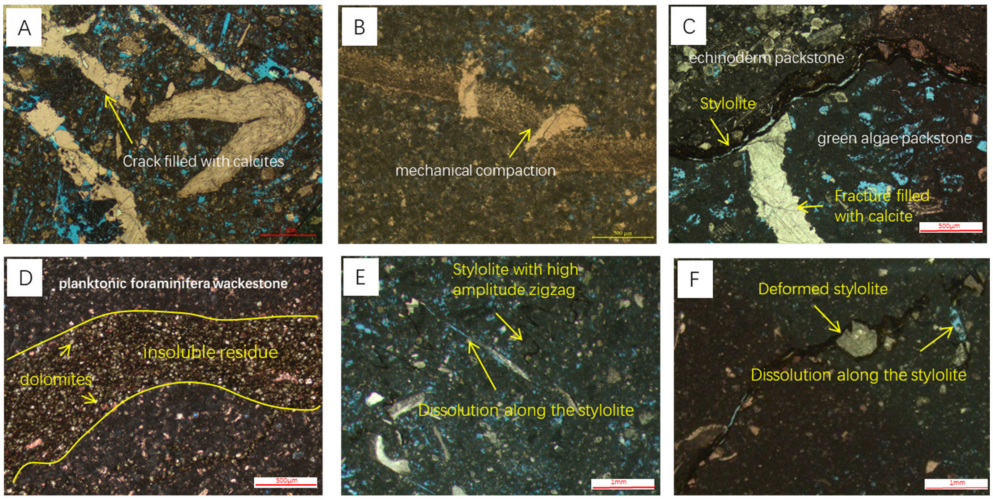

Figure 5. The diagenesis related to the pressure dissolution. (**A**) The irregular cracks in the limestone; (**B**) the compaction of the fossil; (**C**) a weathering crack filled with calcite was cut by a stylolite; (**D**) dolomites in the insoluble residue of dissolution seams; (**E**) a dissolution could be seen at the column of the stylolite; (**F**) the dissolution along the segment of a deformed stylolite in the bioclastic wackestones.

4.3. The Patterns of Stylolites

From the observation of thin sections and cores, there were different patterns of stylolites (Figure 6A–D). The wave-like stylolite with low amplitude could be seen in the mixed lithofacies with echinoderm packstone and green algae packstone (Figure 6A), containing a few insoluble residues. The highly serrate stylolite with high amplitude could

be observed in the green algae packstone, with a few black insoluble residues (Figure 6B). The stylolite with thick insoluble residues could be observed in the bioclastic wackestones (Figure 6C, D). Meanwhile, there were some oblique stylolites on the cores. Oblique stylolites intersected the bedding plane at a high angle, e.g., high-angle stylolite (Figure 7). In terms of the patterns of stylolites, four types of stylolites could be distinguished (Figure 7). Type A was the wave-like stylolite developed at the boundary between the echinoderm packstones and green algae packstones. Type B was the zigzag stylolite with high amplitude in the green algae packstones. Type C included the stylolites with low amplitude in the bioclastic wackestones. Type D was the high-angle stylolite, which was oblique to the bedding plane.

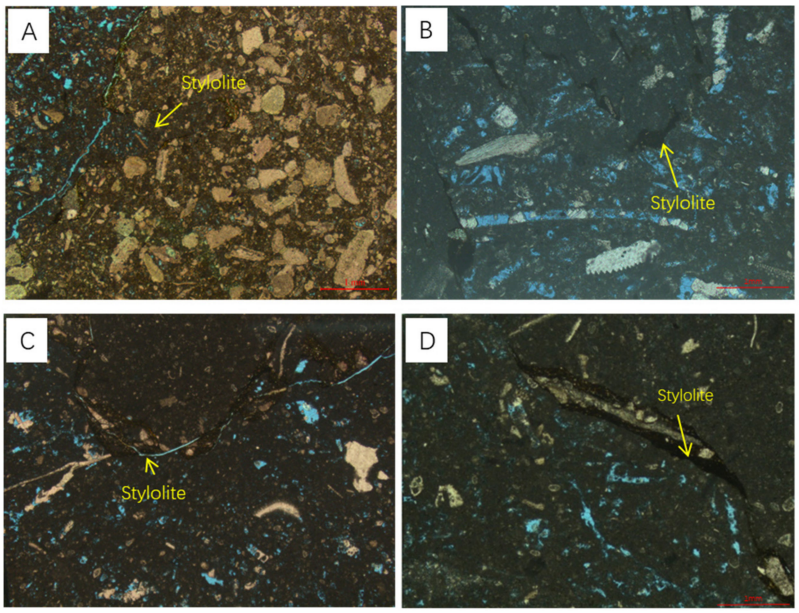

Figure 6. The pressure dissolution features in the thin sections. (**A**) The stylolite developed at the boundary of two lithofacies, type A stylolite; (**B**) the highly serrate stylolite in the green algae packstone, type B stylolite; (**C**,**D**) the low-amplitude stylolite with thick insoluble residues in the bioclastic wackestone, type C stylolite.

The numbers of stylolite have been counted under thin sections. The density of stylolites per meter is shown in Figure 8. There is a large number of stylolites in the Mi4-4 and Mi4-5 lithozones. Type A and type C stylolite are most common under the thin sections and cores.

4.4. Porosity and Permeability

The porosity and permeability of rocks in the study were 6.63–25.6% and 0.06 mD–48.3 mD, respectively. The average porosity of rocks in the Mi4-1, Mi4-4 and Mi4-5 lithozones was lower than 20% (Figure 9). There was relatively low permeability in the Mi4-5 lithozone (Figure 9). The Mi4-2 and Mi4-3 lithozones had relatively high porosity and permeability.

4.5. Analysis of Well Test

In the analysis of the well test, there were multiple platforms in the differential of the pressure curve from four horizontal wells, with the horizontal segment in the Mi4-3 lithozone (well A7-5H, well A5-2H) (Figure 10). When the well trajectory tracked horizontally through the formation (e.g., well A0-3 and well A9-2), the vertical radial flow occurred in less than one hour in the double logarithmic curve (Figure 10), suggesting that baffles may exist in the reservoir. This could be caused by the distribution of stylolites in the Mi4-3 lithozone.

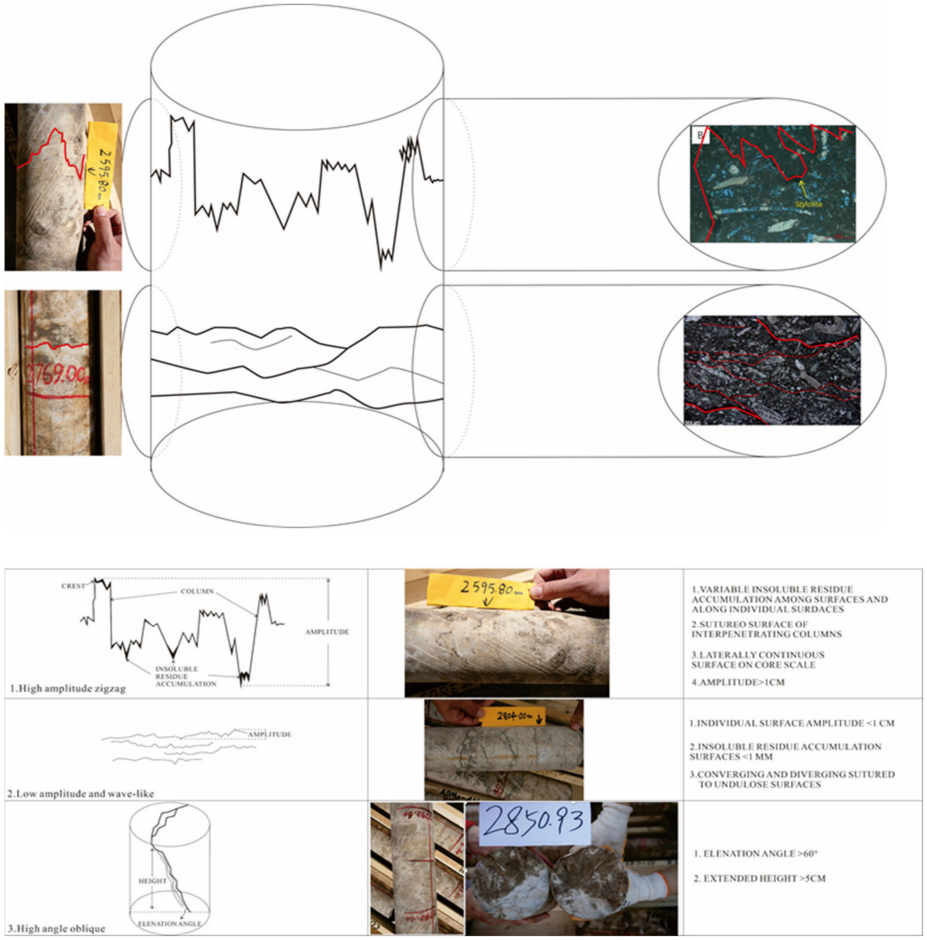

Figure 7. The pattern of stylolite observed on the cores.

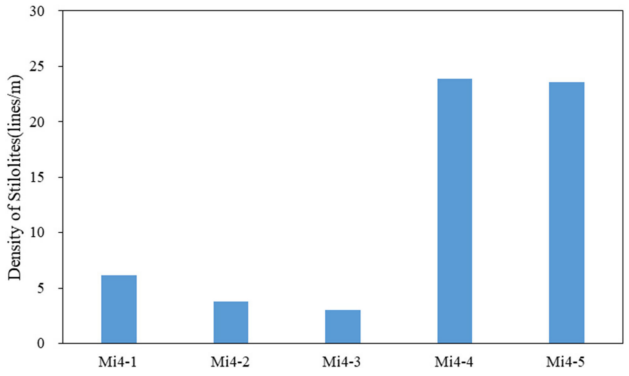

Figure 8. The density of stylolites in the Mi4 member under the thin sections.

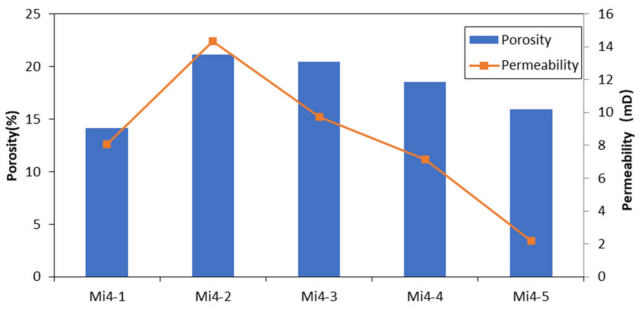

Figure 9. The average porosity and permeability of the Mi4 member.

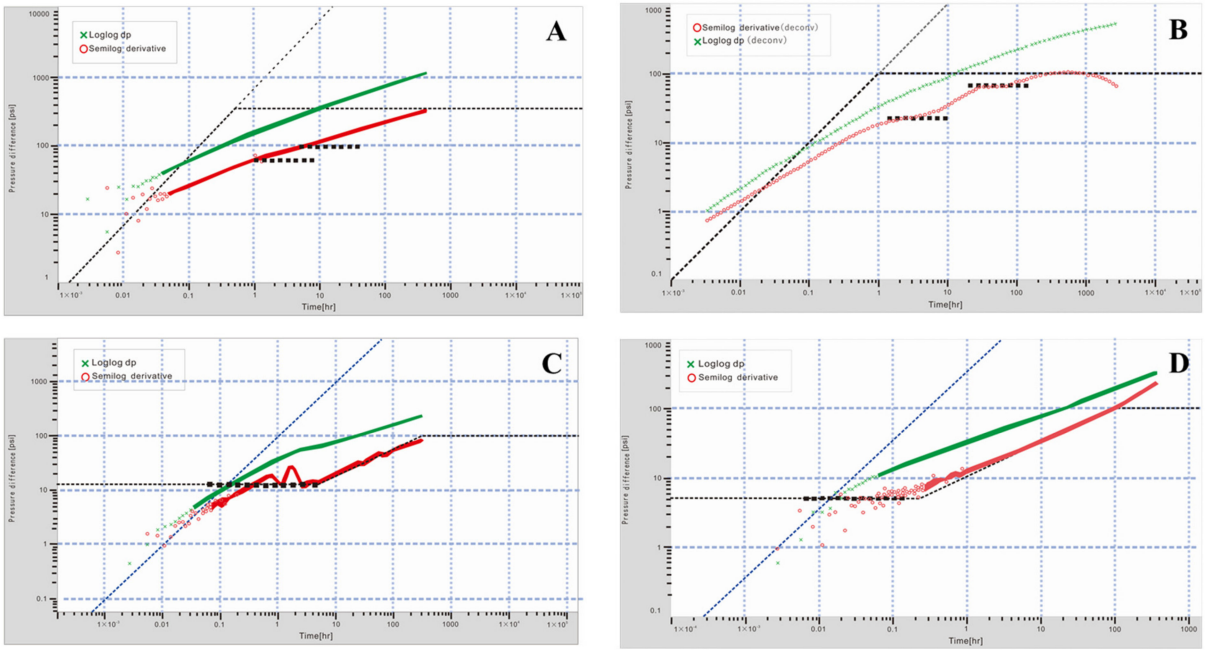

Figure 10. The differential of pressure curves from four horizontal wells. (**A**) A7-5H; (**B**) A5-2H; (**C**) A0-3H; (**D**) A9-2H.

5. Discussion

5.1. The Density of Stylolites Controlled by the Lithofacies and Early Cementation

The development of stylolites on the cores was influenced by the lithofacies and its early cementation. Early cementation was the major limiting factor of compaction and then pressure dissolution [25], as well as the content of rigid particles. In the study, packstones with high content of rigid particles (e.g., skeletal grains) had the greater capacity to resist compaction compared to wackestones. Mechanical compaction and pressure dissolution were concentrated in the less cemented strata [23,26]. In the Mi4 member, there was obvious selective cementation in the various packstones. The early cementation of packstones could occur in the mixed seawater–freshwater phreatic zone and later freshwater phreatic zone, as shown in Figure 4. Based on the statistics of the number of stylolites under thin sections, there was a relatively high frequency of stylolite in the planktonic foraminifera wackestone and bioclastic wackestone (Figure 11). The lack of skeletal grains and early cements in these two lithofacies resulted in the development of stylolites. Boutaleb et al. (2022) also suggest that the stylolite is prone to develop within the planktic foraminiferal wackestone and wackestone–packstone facies [17]. In the study, the highest density of stylolite occurred in Mi4-4 and Mi4-5 with the lithofacies of bioclastic wackestone and planktonic foraminifera wackestones. Type C stylolite with thick insoluble residues developed in these two lithofacies (Figure 6C,D).

There was the highest frequency of stylolite in the mixed facies of echinoderm packstone and bivalve green algae packstone (Figure 11). The mixed facies were formed by bioturbation. The bivalve green algae packstone, as the host rock, mixed with the echinoderm packstone filled in the burrow. There was obvious porosity instability in the interface between echinoderm packstone almost without pores and porous green algae packstone (Figure 6A). The bedding planes between these lithofacies could have improved the formation of a stylolite c.f. [7]. Type A stylolites were developed at the boundary between these two lithofacies, and they were common in the Mi4 member.

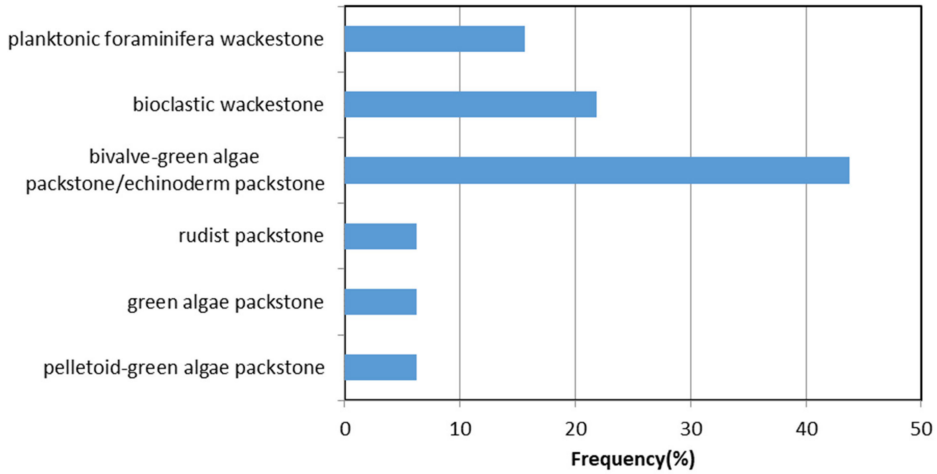

Figure 11. The frequency of stylolite in the different lithofacies.

There was a low frequency of stylolites in the rudist packstone, green algae packstone and pelletoid green algae packstone (Figure 11). Because of the high content of skeletal grains and relatively greater number of early cements (almost 3~13% content of early calcite), stylolites are rare in the above packstones. In these packstones, type B stylolite could be observed.

In a previous study, it was suggested that the clay minerals could improve the pressure dissolution where the stress is low [27,28]. The clay minerals will deposit together with the formation of micrite, under a relatively low-energy environment. There are much larger amounts of micrite in wackestones than in packstones, leading to the clay mineral content being relatively high in wackestones. However, the clay mineral content in the whole rock was found to be less than 1% by XRD measurement. Although the clay minerals have not been detected by XRD, the clay, terrigenous quartz and organic matter within stylolites could be observed under the thin sections. The clay minerals within the matrix-supported wackestone might be another factor to induce the formation of stylolite.

As a result, the different density of stylolite in the Mi4 member was mainly controlled by the lithofacies and the different degrees of early cementation.

5.2. The Stress Controls the Distribution of Stylolite

The pressure dissolution process is affected by many factors. The most important factor is stress. The relevant models include the anti-crack concept [29] and the dislocation model [30,31]. Therefore, stylolites can grow at the tip of fracture. The stylolite can be used to calculate overburden or tectonic stresses [32,33]. The filtering effect of rock itself can control the pressure solution occurring on the free surface of particles, leading to an increase in stress and promoting further pressure solution [7]. Differences in the direction of the stress will result in stylolites with different patterns. With the formation of an anticline structure in the Ah Oilfield, the stress in the flank of the anticline will increase and produce horizontal interlayer shearing fractures, which are parallel to the bedding of rocks. These fractures provide the foundation for pressure dissolution. The dissolved substances will migrate along the fractures with the increase in the overburden stress. As a result, the number of stylolites in the Mi4 member of well AH-4H in the core of the anticline is less than that in well AH-8H in the steep flank of the anticline. Meanwhile, type D stylolite is only distributed on the core from well AH-4H. However, the cementation before the pressure dissolution could influence the stress concentration during the pressure compaction, resulting in a decrease in porosity instability. As shown in Table 2, the number of stylolites in well AH-1H with strong cementation is lower than at other sites.

Table 2. The number of stylolites in the Mi4 member in Ah Oilfield.

Well	**AH-4H**	**AH-8H**	**AH-1H**
Structure Site	Core of Anticline	Steep Flank of Anticline	Gentle Flank of Anticline
Mi4-1	11	11	11
Mi4-2	15	4	3
Mi4-3	1	20	2
Mi4-4	45	81	27
Mi4-5	30	55	14
Total	102	171	57

The pattern of stylolite has a close relationship with the direction of stress. Type A, B and C stylolites are approximately parallel to the bedding. The horizontal shearing force and later overburden pressure are responsible for the formation of type A, B and C stylolites. Type C stylolites are oblique to the bedding at a high angle, resulting from the later lateral compression. The compression occurred at the Late Cretaceous and the Late Miocene [20]. At the two stages, the thickness of the sediment column above the Mishrif Formation was approximately 550 m and 2920 m. As the pressure dissolution occurred at least beyond 1000 m, the timing of the formation of type D stylolite was the Late Miocene. During the compression in the late diagenesis, compaction and dissolution will also occur between two lithofacies with distinct porosity. The lithofacies' boundaries, with different directions, are very likely controlled by the bioturbation in the study area, leading to the boundary of two lithofacies not being parallel to the bedding plane.

5.3. The Effect of Stylolite on the Petro-Physical Properties of Reservoir Rock

The stylolite could act as fluid flow channels or baffles, resulting in a change in permeability in the vertical direction [34,35]. As discussed above, stylolite could act as the fluid flow channel when the column of stylolite develops, e.g., type B stylolite. In previous studies, zigzag stylolites with high amplitude were regarded to improve permeability [34,36–40]. Enhanced dissolution along the column of stylolite can enhance permeability [41,42]. Therefore, type B stylolite could improve the permeability in the lithofacies. However, the low amplitude of type A and C stylolite results in the absence of a column, leading to the thick insoluble residues within the stylolite. As a result, the stylolites act as fluid flow baffles. If the stylolite plane only contains less residual substances, it is possible to allow liquid to flow. Type A stylolites are the most common stylolites in the Mi4 member. Due to the various degrees of compaction and dissolution during the formation of Type A, the influence of type A stylolite on the permeability is not clear. Type D stylolite, with a high angle, could play the role of baffle in the horizontal direction of fluid flow. In the vertical direction, type D stylolite could be the fluid flow channel, as the stylolite plane will be open in the tensional stress. There was abundant oil enrichment in the high-quality reservoir near the type D stylolite (Figure 6).

Due to the different original porosity of each lithofacies, it was suggested that the effect of stylolite on the porosity and permeability of reservoir rocks in the Mi4 member was related to the type of lithofacies in the study. The comparison between the petro-physical properties of lithofacies with and without stylolite is shown in Figure 12. The development of stylolite could result in a decrease in the permeability of green algae packstone and echinoderm packstone. As the stylolite is prone to occur at the interface between green algae packstone and echinoderm packstone with porosity instability, the stylolite will act as a fluid baffle to reduce the permeability. Therefore, the permeability of green algae packstone and echinoderm packstone will decrease during the formation of stylolites. The porosity and permeability of bivalve green algae packstone will decrease at the same time with the development of stylolites. There was strong compaction and dissolution in the bivalve green algae packstone with a large amount of stylolite residues (Figures 5 and 6). In addition, the porosity and permeability of bioclastic wackestone could be improved by bioturbation, followed by pressure dissolution at the interface between the host rock and

bioturbation fillings. Therefore, the stylolite could impact the petro-physical properties of reservoir rocks, which are controlled by the lithofacies and the original porosity instability.

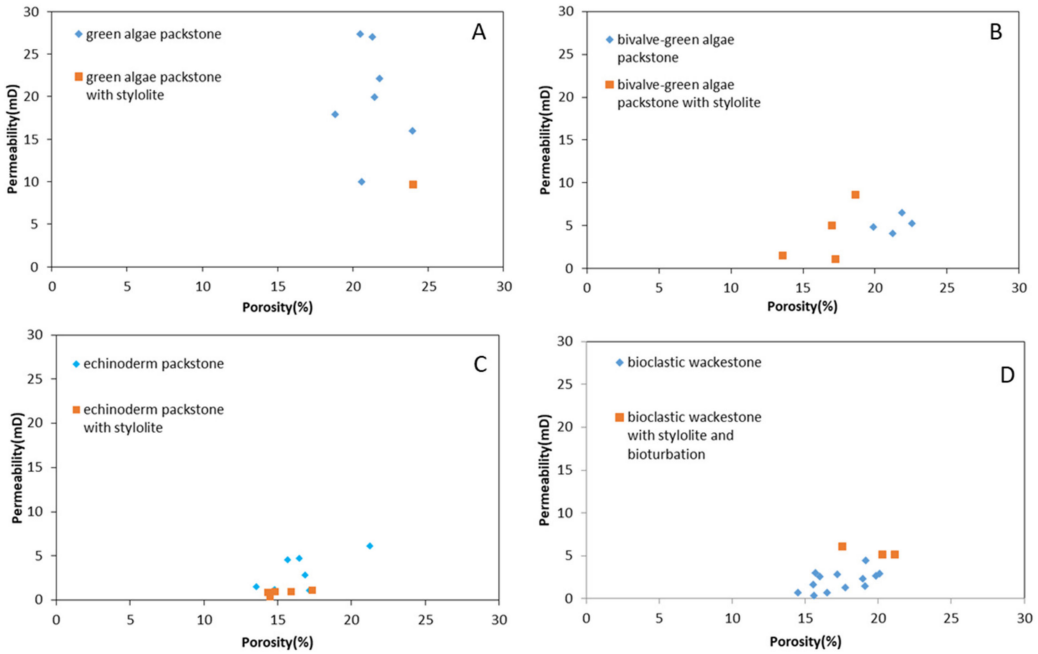

Figure 12. The cross-plot of porosity and permeability of limestones without or with stylolite in the Mi4 member: (**A**) green algae packstone; (**B**) bioclastic green algae packstone; (**C**) echinoderm packstone; (**D**) bioclastic wackestone.

5.4. The Influence of Stylolite on the Production Performance

As the development of stylolite could result in the formation of fluid flow barriers in some cases [43], the interval with high-density stylolite may represent a baffle between oil zones. However, the study by Al-Amrie et al. (2012) suggested that the stylolite zones have no sealing capacity for fluid flow, which was shown using vertical interference tests in a newly drilled well [44]. In the study, the influence of stylolite on the production performance was discussed. As shown in Figure 10, the occurrence of a platform in the differential of pressure curve shows that there are some oil baffles in the Mi4-3 lithozone. Meanwhile, as for well A0-3 and well A9-2, with the well trajectory tracking horizontally through the formation, the vertical radial flow occurs in less than one hour (Figure 10), which indicates that the thickness of the flow through porous media is less than the thickness of the lithozone. The sites of well A0-3 and well A9-2 are located at the flank of the anticline, implying that the density of the stylolite could be relatively high. Because the lithofacies of Mi4-3 lithozone are similar (e.g., bivalve green algae packstone), a change in the density of stylolite and the associated cementation related to pressure compaction could result in the development of oil baffles, leading to different production performance.

6. Conclusions

(1) The pattern of stylolite has a close relationship with the direction of stress. The number of stylolites in the Mi4 member in the core of the anticline is less than that in the steep flank of the anticline.

(2) The effect of stylolite on the physical properties of packstone and wackestone is related to the lithofacies and the density of the stylolite. The porosity and permeability of bivalve green algae packstone will decrease at the same time after stylolitization, resulting from the relatively high density of stylolite.

(3) The density change of stylolite in the same lithofacies could result in the development of an oil baffle, leading to different production performance.

Author Contributions: Conceptualization, Y.D.; methodology, M.F.; software, P.C.; Validation, G.D.; investigation, R.M.; resources, Y.D.; data curation, M.F.; writing—original draft preparation, J.X.; writing—review and editing, J.X.; visualization, P.C.; supervision, R.G.; project administration, R.G.; funding acquisition, Y.D. All authors have read and agreed to the published version of the manuscript.

Funding: China national petroleum co., LTD. " 14th five years" forward-looking basic major s&t projects, "extra low permeability carbonate reservoir in the effective development of key technology research".

Institutional Review Board Statement: Not applicable.

Informed Consent Statement: Not applicable.

Data Availability Statement: Not applicable.

Conflicts of Interest: The authors declare that they have no known competing financial interests or personal relationships that could have appeared to influence the work reported in this paper.

References

1. Amstutz, G.C.; Park, W.C. Stylolites of diagenetic age and their role in the interpretation of the southern Illinois fluorspar deposits. *Miner. Depos.* **1967**, *2*, 44–53. [CrossRef]
2. Burgess, C.J.; Peter, C.K. Formation, Distribution and Prediction of Stylolites as Permeability Barriers in the Thamama Group, Abu Dhabi. Presented at the Middle East Oil Technical Conference and Exhibition, Manama, Bahrain, 11–14 March 1985.
3. Dunnington, H.V. Aspects of Diagenesis and Shape Change in Stylolitic Reservoirs. In Proceedings of the Seventh World Petroleum Congress, Mexico City, Mexico, 2–9 April 1967; pp. 339–352.
4. Logan, B.W.; Semeniuk, V. *Dynamic Metamorphism, Processes and Products in Devonian Carbonate Rocks, Canning Basin, Western Australia*; Special Publication 6; Geology Sociation of Australia: Sydney, Australia, 1976; pp. 138–145.
5. Dürast, H.; Siegesmund, S. Correlation between rock fabrics and physical properties of carbonate reservoir rocks. *Int. J. Earth Sci.* **1999**, *88*, 392–408. [CrossRef]
6. Koepnick, R.B. Distribution and Permeability of Stylolite-Bearing Horizons Within a Lower Cretaceous Carbonate Reservoir in the Middle East. *SPE Form. Eval.* **1985**, *2*, 137–142. [CrossRef]
7. Merino, E.; Ortoleva, P.; Strickholm, P. Generation of evenly-spaced pressure-solution seams during (late) diagenesis: A kinetic theory. *Contrib. Mineral. Petrol.* **1983**, *82*, 360–370. [CrossRef]
8. Koehn, D.; Rood, M.P.; Beaudoin, N.; Chung, P.; Bons, P.D.; Gomez-Rivas, E. A new stylolite classification scheme to estimate compaction and local permeability variations. *Sediment. Geol.* **2016**, *346*, 60–71. [CrossRef]
9. Borgen, V.D.; Carozi, A.V. Experimentally-simulated styloliticporosity in carbonate rocks. *J. Pet. Geol.* **1990**, *13*, 179–192. [CrossRef]
10. Hu, M.; Zhu, Z.; Liu, B. Diagenesis and pore evolution of carbonate rocks of the Ordovician in the middle An-hui. *Minerology* **1994**, *14*, 47–54.
11. Ma, Y.; Tian, H.; Chen, H.; Mao, C.; Cai, X. *Carbonate Rock Microfacies: Analysis, Interpretation & Application*; Geology Press: Beijing, China, 2006; pp. 296–302.
12. Zhou, D.; Li, G.; Luo, P.; Zhang, D.; Tang, H. Diagenesis research of Shiniulan Group of the Silurian in the southeastern Sichuan. *Nat. Gas Technol.* **2009**, *3*, 6–11.
13. Ramsdom, R.M. Stylolites and oil migration. *AAPG Bull.* **1952**, *36*, 2185–2186.
14. Zhong, J.; Kong, F.; Li, Y.; Yuan, X. Stylolite research of the Ordovician carbonate reservoir in the forth area of Tahe oil field. *Geol. Rev.* **2010**, *5*, 841–850.
15. He, B. Oil sepage and bitumen in Guangxi area. *J. Beijing Geol. Inst.* **1959**, *5*, 8–13.
16. Boutaleb, K.; Baouche, R.; Sadaoui, M.; Radwan, A.E. Sedimentological, petrophysical, and geochemical controls on deep marine unconventional tight limestone and dolostone reservoir: Insights from the Cenomanian/Turonian oceanic anoxic event 2 organic-rich sediments, Southeast Constantine Basin, Algeria. *Sediment. Geol.* **2022**, *429*, 106072. [CrossRef]
17. Bai, G. Relation Between Stylolite and Reservoir in Moxi Gasfield. *Oil Gas Geol.* **1992**, *13*, 418–422.
18. Aqrawi, A.A.M.; Goff, J.C.; Horbury, A.D.; Sadooni, F.N. *The Petroleum Geology of Iraq Beaconsfield*; Scientific Press: Bucks, UK, 2010; p. 424.
19. Aqrawi, A.A.M.; Thehni, G.A.; Sherwani, G.H.; Kareem, B.M.A. Mid-Cretaceous Rudist-Bearing carbonates of the Mishrif Formation: An important reservoir sequence in the Mesopotamian Basin, Iraq. *J. Pet. Geol.* **1998**, *21*, 57–82. [CrossRef]
20. Deng, H.; Fu, M.; Huang, T.; Gluyas, J.G.; Tong, M.; Wang, X.; Zhou, W.; Liu, F. Ahdeb oil field, Mesopotamian Basin, Iraq: Reservoir architecture and oil charge history. *AAPG Bull.* **2018**, *102*, 2447–2480. [CrossRef]
21. Jannot, Y.; Lasseux, D. A new quasi-steady method to measure gas permeability of weakly permeable porous media. *Rev. Sci. Instrum.* **2012**, *8*, 2015–2113. [CrossRef]
22. Li, C.; Zhao, L.; Li, W.; Li, J.; Ding, Y.; Li, Y.; Qi, Y. Research status and its significance to oil-field development of stylolite in car bonate. *Nat. Gas Geosci.* **2019**, *30*, 493–502.

23. Railsback, L.B. Contrasting styles of chemical compaction in the Upper Pennsylvanian dennis limestone in the Midcontinent region, U.S.A. *J. Sediment. Res.* **1993**, *63*, 61–72.
24. Machel, H.G. Concepts and models of dolomitization: A critical reappraisal. *Geol. Soc. Lond. Spec. Publ.* **2004**, *235*, 7–63. [CrossRef]
25. Clari, P.A.; Martire, L. Interplay of cementation, mechanical compaction, and chemical compaction in nodular limestones of the Rosso Ammonitico Ceronese (Middle-Upper Jurassic, Northeastern Italy). *J. Sediment. Res.* **1996**, *66*, 447–458.
26. Bathurst, R.G.C. Diagenetically enhanced bedding in argillaceous platform limestones: Stratified cementation and selective compaction. *Sedimentology* **1987**, *34*, 749–778. [CrossRef]
27. Aharonov, E.; Katsman, R. Interaction between pressure solution and clays in stylolite development: Insights from modeling. *Am. J. Sci.* **2009**, *309*, 607–632. [CrossRef]
28. Katsman, R. Extensional veins induced by self-similar dissolution at stylolites: Analytical modeling. *Earth Planet. Sci. Lett.* **2010**, *299*, 33–41. [CrossRef]
29. Fletcher, R.C.; Pollard, D.D. Anti-Crack Model for Pressure Solution Surfaces. *Geology* **1981**, *9*, 419–424. [CrossRef]
30. Katsman, R.; Aharonov, E.; Scher, H. Localized compaction in rocks: Eshelby's inclusion and the Spring Network Model. *Geophys. Res. Lett.* **2006**, *33*, L10311. [CrossRef]
31. Katsman, R.; Aharonov, E.; Scher, H. A numerical study on localized volume reduction in elastic media: Some insights on the mechanics of anticracks. *J. Geophys. Res.-Solid Earth* **2006**, *111*, B03204. [CrossRef]
32. Schmittbuhl, J.; Renard, F.; Gratier, J.P.; Toussaint, R. Roughness of stylolites: Implications of 3D high resolution topography measurements. *Phys. Rev. Lett.* **2004**, *93*, 238501. [CrossRef] [PubMed]
33. Beaudoin, N.; Koehn, D.; Lacombe, O.; Lecouty, A.; Billi, A.; Aharonov, E.; Parlangeau, C. Fingerprinting stress: Stylolite and calcite twinning paleopiezometry revealing the complexity of progressive stress patterns during folding-the case of the Monte Nero anticline in the Apennines, Italy. *Tectonics* **2016**, *35*, 1687–1712. [CrossRef]
34. Carozzi, A.V.; Vonbergen, D. Stylolitic Porosity in Carbonates—A Critical Factor for Deep Hydrocarbon Production. *J. Pet. Geol.* **1987**, *10*, 267–282. [CrossRef]
35. Alsharhan, A.; Sadd, J.L. *Stylolites in Lower Cretaceous Carbonate Reservoirs, U.A.E.//Middle East Models of Jurassic/Cretaceous Carbonate Systems*; Special Publication; SEPM (Society for Sedimentary Geology): Broken Arrow, OK, USA, 2000; Volume 69, pp. 185–207. Available online: https://pubs.geoscienceworld.org/sepm/books/book/1375/chapter/10792706/Stylolites-in-Lower-Cretaceous-Carbonate (accessed on 26 March 2022).
36. Dawson, W.C. Stylolite porosity in carbonate reservoirs: American Association of Petroleum Geologists Search and Discovery Article. In Proceedings of the American Association of Petroleum Geologists Annual Convention, Houston, TX, USA, 20–23 March 1988.
37. Raynaud, S.; Carrio-Schaffhauser, E. Rock Matrix Structures in a Zone Influenced by a Stylolite. *J. Struct. Geol.* **1992**, *14*, 973–980. [CrossRef]
38. Van Geet, M.; Swennen, R.; Wevers, M. Quantitative analysis of reservoir rocks by microfocus X-ray computerised tomography. *Sediment. Geol.* **2000**, *132*, 25–36. [CrossRef]
39. Gingras, M.K.; MacMillan, B.; Balcom, B.J. Visualizing the internal physical characteristics of carbonate sediments with magnetic resonance imaging and petrography. *Bull. Can. Pet. Geol.* **2002**, *50*, 363–369. [CrossRef]
40. Harris, N.B. Low-Porosity Haloes at Stylolites in the Feldspathic Upper Jurassic Ula Sandstone, Norwegian North Sea: An Integrated Petrographic and Chemical Mass Balance Approach. *J. Sediment. Res.* **2006**, *76*, 444–459. [CrossRef]
41. Ben-Itzhak, L.L.; Aharonov, E.; Karcz, Z.; Kaduri, M.; Toussaint, R. Sedimentary stylolite networks and connectivity in limestone: Large-scale field observations and implications for structure evolution. *J. Struct. Geol.* **2014**, *63*, 106–123. [CrossRef]
42. Rustichelli, A.; Tondi, E.; Korneva, I.; Baud, P.; Vinciguerra, S.; Agosta, F.; Reuschlé, T.; Janiseck, J.M. Bedding-parallel stylolites in shallow-water limestone successions of the Apulian Carbonate Platform (central-southern Italy). *Ital. J. Geosci.* **2015**, *134*, 513–534. [CrossRef]
43. Al-Ansari, F.; Konwar, L.S.; Urasaki, D.; Parker, A.; Hiraoka, T.; Mitsuishi, H. Vertical transmissibility assessment across stylolites in stratified carbonate reservoir—A Field Experience. Presented at the 9th Abu Dhabi International Petroleum Exhibition and Conference, Abu Dhabi, United Arab Emirates, 1–10 October 2000. SPE 87301.
44. Al-Amrie, O.Y.; Mohamed, A.B.S.; Al Marzouqi, K.I.; Kshirsagar, A.; Coskun, S.B. The use of a formation tester to characterize permeability and vertical communication across stylolite zones in a carbonate reservoir-Case study. Presented at the Abu Dhabi International Petroleum Exhibition & Conference, Abu Dhabi, United Arab Emirates, 11–14 November 2012. SPE 160956.